Translational Oncology 13 (2020) 100844

Contents lists available at ScienceDirect

Translational Oncology

journal homepage: www.elsevier.com/locate/tranon

Original research

Downstream neighbor of SON (*DONSON*) is associated with unfavorable survival across diverse cancers with oncogenic properties in clear cell renal cell carcinoma

Niklas Klümper [a,b,c,*], Iulia Blajan [a,b], Doris Schmidt [a,b], Glen Kristiansen [b,d], Marieta Toma [b,d], Michael Hölzel [b,c], Manuel Ritter [a,b], Jörg Ellinger [a,b]

[a] Department of Urology, University Hospital Bonn, Bonn, Germany
[b] Center for Integrated Oncology, University Hospital Bonn, Bonn, Germany
[c] Institute of Experimental Oncology, University Hospital Bonn, Bonn, Germany
[d] Institute for Pathology, University Hospital Bonn, Bonn, Germany

ARTICLE INFO

Article history:
Received 4 June 2020
Received in revised form 6 July 2020
Accepted 9 July 2020
Available online xxxx

ABSTRACT

A precise stratification of our patients is essential and can support clinicians to determine the right therapy. The aim of this study was to identify clinically relevant genes using The Cancer Genome Atlas (TCGA) datasets.
A comprehensive pan-cancer analysis of 30 distinct tumor entities ($N = 9022$) identified the largely unknown gene Downstream neighbor of SON (DONSON) to be particularly associated with unfavorable overall survival in clear cell renal cell carcinoma (KIRC). This prognostic potential of DONSON was validated in an independent KIRC cohort via quantitative real-time PCR (n = 152). Further, DONSON protein expression was evaluated via immunohistochemical staining followed by quantitative image analysis using the image analysis software QuPath on a renal cancer tissue microarray (n = 270).
Interestingly, DONSON overexpression was preferentially associated with poor survival in 9 of the 30 entities, suggesting tumor-independent oncogenic properties of this largely unknown gene. A particularly strong association of DONSON to an aggressive phenotype was evident in KIRC and proved to be a strong independent predictor of unfavorable overall survival in two additional cohorts on the mRNA and protein level. In our KIRC cell culture model, we observed a substantial attenuation of proliferative activity and migration capacity of the KIRC cells Caki1 and 769p.
In conclusion, we identified DONSON as a robust biomarker for risk stratification in KIRC in three independent cohorts and provide evidence that DONSON is linked to a malignant phenotype in the KIRC cell culture model.

Introduction

Renal cell carcinoma (RCC) is the most prevalent malignant kidney lesion in adults, with continuously increasing incidence [1,2]. The major histological subtypes in descending order include clear cell RCC in about 80% (KIRC), followed by papillary RCC (KIRP) and chromophobe (KICH) [3]. In metastatic RCC, the clinical implementation of multi-tyrosine kinase inhibitors (TKI) and immune checkpoint inhibitors (ICI), led to an improved clinical outcome [4–8]. However, many patients do not respond or ultimately develop resistance under these treatment regimens. Thus, the identification of diagnostic and prognostic biomarkers, based on molecular tumor characteristics, is essential for predicting tumor aggressiveness and improved therapeutic management tailored to individualized therapy approaches.

Publicly available genomic databases, such as The Cancer Genome Atlas (TCGA) have become essential tools in cancer research [9–11]. In a systematic multivariate Cox regression analysis, the relatively unknown Downstream neighbor of SON (DONSON) was found as a particularly strong predictor for unfavorable overall survival in the KIRC, which prompted us to examine this gene more closely [12,13]. DONSON has previously been identified as a replisome component, responsible for fork stabilization during genomic replication [14]. Overall, DONSON plays a crucial role in maintaining genomic integrity, cell cycle progression, and efficient replication [15]. Regarding cancer research, not much was known about DONSON until very recently.

A MicroRNA (miRNA) passenger strand, *miR101-5p*, acting tumor suppressive in RCC, was found to directly regulate the DONSON expression. Ectopic expression of *miR101-5p*, as well as a siRNA-mediated DONSON-knockdown, attenuated the malignant features of RCC cells [16].

However, the implications of DONSON in KIRC pathogenesis and tumor progression, as well as its value as a promising biomarker for patient stratification, are not yet fully characterized.

* Corresponding author at: Clinic for Urology and Pediatric Urology, University Hospital Bonn, Venusberg-Campus 1, 53127 Bonn, Germany.
E-mail address: niklas.kluemper@ukbonn.de. (N. Klümper).

http://dx.doi.org/10.1016/j.tranon.2020.100844

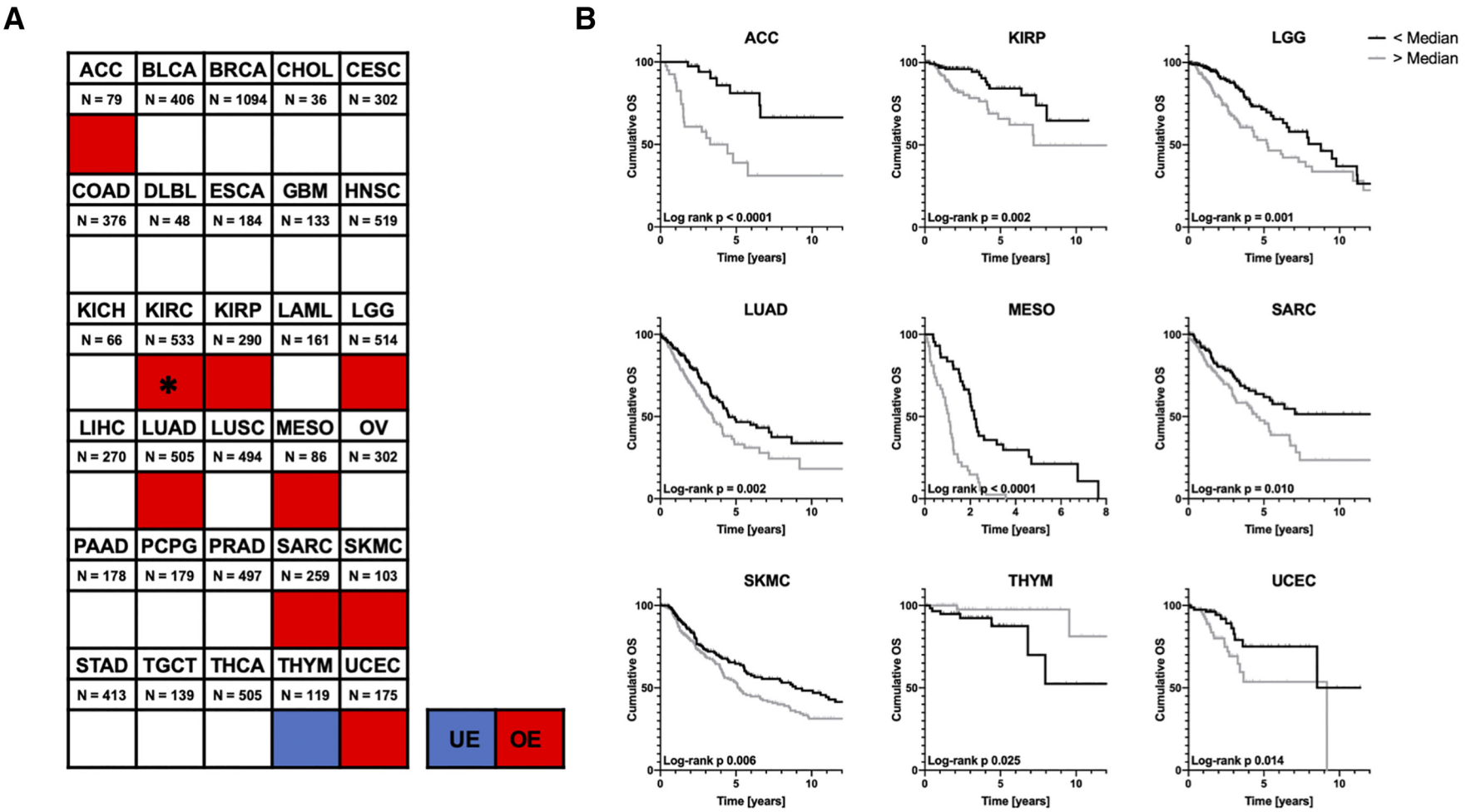

Fig. 1. A, Heatmap of the prognostic value of DONSON in 30 different tumor entities using log-rank tests after median dichotomization (N = 9022); standard TCGA study abbreviations were used; red/OE = high expression, blue/UE = low expression. Tumor abbreviations: ACC = adrenocortical carcinoma, BLCA = bladder urothelial carcinoma, BRCA = breast invasive carcinoma, CHOL = cholangiocarcinoma, CESC = cervical squamous cell carcinoma and endocervical adenocarcinoma, COAD = colon adenocarcinoma, DLBL = lymphoid neoplasm diffuse large B-cell lymphoma, ESCA = esophageal carcinoma, GBM = glioblastoma multiforme, HNSC = head and neck squamous cell carcinoma, KICH = kidney chromophobe carcinoma, KIRC = kidney renal clear cell carcinoma, KIRP = kidney renal papillary carcinoma, LAML = acute myeloid leukemia, LGG = brain lower grade glioma, LIHC = liver hepatocellular carcinoma, LUAD = lung adenocarcinoma, LUSC = lung squamous cell carcinoma, MESO = mesothelioma, OV = ovarian serous cystadenocarcinoma, PAAD = pancreatic adenocarcinoma, PCPG = pheochromocytoma and paraganglioma, PRAD = prostate adenocarcinoma, SARC = sarcoma, SKMC = skin cutaneous melanoma, STAD = stomach adenocarcinoma, TGCT = testicular germ cell tumors, THCA = thyroid carcinoma, THYM = thymoma, UCEC = uterine corpus endometrial carcinoma. B, Significant associations between DONSON expression and unfavorable overall survival across the TCGA cohorts are depicted as Kaplan-Meier estimate curves. (For interpretation of the references to color in this figure legend, the reader is referred to the web version of this article.)

Methods

TCGA data

The UCSC Xena browser (http://xena.ucsc.edu) was used to download TCGA transcriptome sequencing data (Log2 transformed RNA-Seq v2) for DONSON in 30 different tumor types (see Fig. 1A, $N = 9022$, including KIRC $N = 532$, plus normal adjacent kidney tissue (NAT) $N = 72$) [12].

RCC cohorts of the University Hospital Bonn (UHB)

Via the Biobank at the University Hospital Bonn fresh-frozen or formalin-fixed paraffin-embedded paraffin (FFPE) RCC tissue samples were assembled as a KIRC cDNA cohort and KIRC tissue microarray as described previously [17,18]. All patients provided written informed consent before the specimens were collected in accordance with the declaration of Helsinki.

RNA isolation and real-time PCR

50 mg of cryo-preserved tissue was homogenized, and the total RNA was isolated using the mirVana miRNA Isolation Kit (Ambion, Foster City, CA, USA) as described previously [17,18] (KIRC $N = 103$, NAT $N = 20$). The DNA elimination was achieved by treatment of the RNA with DNase (DNA-free Kit, Ambion).

The RNA of the cell lines was isolated from pellets using the Total RNA Purification Mini Spin Column Kit (Genaxxon bioscience GmbH, Ulm, DE). The RNA quantity and quality were determined using the NanoDrop 2000 Spectrophotometer (Thermo Scientific, Wilmington, DE, USA).

Reverse transcription of approximately 1 μg total RNA was performed using the PrimeScript RT Reagent Kit with gDNA Eraser. The *DONSON*-knockdown validation PCR experiments were carried out following genomic DNA elimination by treating 1 μg of total RNA with gDNA Eraser for 2 min at 42 °C and subsequent reverse transcription with the same PrimeScript RT Reagent Kit. 5 ng of the resulting cDNA was used for real-time PCR (1× SYBR Premix Ex Taq II with ROX Plus and 10 pmol/μl PCR primers; all reagents: Takara Bio, Saint-Germain-en-Laye, France).

The following primer sequences were used: *DONSON* forward: 5′-GTCC AGCATTGTAGGGCAAC-3′ and reverse: 5′-GGCTCTGCTGGAAGGTACAA-3′, *β-Actin* forward: 5′-CCAACCGCGAGAAGATGA-3′ and reverse: 5′-CCAG AGGCGTACAGGGATAG-3′. The primer annealing temperature was 60 °C for both primer pairs.

Western Blot

For the Western Blot of 8 paired NAT and KIRC samples, approximately 50 mg tissue was homogenized in a Precellys 24 homogenizer (Peqlab, Erlangen, Germany) with 400 μl Cell Lysis Buffer (Cell Signaling, Cambridge, United Kingdom) including protease inhibitor (Complete Mini EDTA-free, Roche, Basel, Switzerland). Each 30 ng protein per lane was separated on a NuPAGE 4–12% Gel in an XCell4 SureLock electrophoresis system (Life Technologies, Carlsbad, CA, USA).

For the Western Blot confirming the DONSON-knockdowns, cells were collected 72 h post-transfection and centrifuged to cell pellets. These were washed with buffered saline (Gibco DPBS, Thermo Fisher Scientific, Waltham, MA, USA) and homogenized in 50 μl of the same cell lysis buffer with a protease inhibitor as stated above. The protein concentration was quantified using a BCA protein assay kit (Thermo Fisher Scientific, Inc., Waltham, MA, USA). Each 20 μg protein per lane was then loaded in a NuPAGE 4–12% Bis Tris Midi Gel. The proteins were transferred on 0.2 μm nitrocellulose (iBlot Gel Transfer Stacks and iBlot Dry Blotting System- Life Technologies), and the non-specific protein binding sites were blocked with a 5% non-fat milk in TBST (50 mM Tris, 150 mM NaCl, 0.05% Tween-20, pH 7.5) for 60 min. The following primary antibodies were used and left to incubate overnight: DONSON 1:1000 (LS-C167506, LifeSpan BioSciences, Seattle, WA, USA) and alpha-Tubulin 1:4000 (T-6074, Sigma Aldrich, Saint Louis, MO, USA). Afterward, the membranes were washed with TBST three times for 5 min, then incubated using horseradish peroxidase-associated secondary antibodies (antirabbit POD, # 7074 Cell Signaling Technology, Danvers, MA, USA and anti-mouse-POD, # 170-6516, Bio-Rad, Hercules, CA, USA). The chemiluminescence signal was depicted with the WesternBright ECL Spray (K-12049-D50, Advansta, San Jose, USA) and documented with a LAS 3000 Image Reader (Fujifilm, Tokyo, Japan).

Immunohistochemistry

DONSON protein expression was investigated using a clinically annotated TMA from paraffin-embedded renal and cancerous tissue as described previously (KIRC $N = 124$, KIRP $N = 29$, KICH $N = 10$, NAT $N = 21$) [17,18]. 5 μm thick paraffin sections were stained with the specific polyclonal DONSON antibody in a 1:50 dilution (HPA039558, Atlas Antibodies, Bromma, Sweden) using the Ventana Benchmark automated staining system (Ventana Medical System, Tuscon, AZ, USA) as formerly described [19,20].

The DONSON protein expression was quantified as an H-score with the semi-quantitative QuPath image analysis software [21]. First, the morphology of the RCC was trained to the algorithm in order to get the automated recognition of the tumor samples with evaluation of the DONSON expression as H-score in the second step.

Cell lines and culture conditions

The RCC cell lines ACHN, CAKI1 and 769p were cultured under standard conditions 5% CO_2/95% air at 37 °C. The 769p and ACHN cell lines were maintained in RPMI1640 medium (Gibco; Thermo Fisher Scientific, Inc., Waltham, MA, USA) while the CAKI1 cell line was cultured in McCoy's 5A medium (Gibco; Thermo Fisher Scientific, Inc., Waltham, MA, USA), both supplemented with 10% fetal bovine serum (FBS Superior, Biochrom GmbH, Berlin, Germany), 0,4% penicillin/streptomycin and only the RPMI1640 medium supplemented with 1% glutamine (Thermo Fisher Scientific, Inc., Darmstadt, Germany). All experiments were performed with mycoplasma-free cells, which have been authenticated before the study began.

Antisense locked nucleic acids (LNA) GapmeR-mediated knockdown

Transfections in the cell lines were performed using a quantity of 10 μl/well for 6-well plates and 0,5 μl/well for 96-well plates with a final concentration of 10 pmol/μl Antisense LNA GapmeR (QIAGEN, Hilden, DE) and FuGENE HD-Transfection reagent (#E2311, Promega Corporation, Madison, WI, USA) in a ratio of 1:1 according to the manufacturer's instructions. The following *DONSON* GapmeR sequence was used (5′–3′): A*C*C*A*G*T*C*A*C*T*C*A*T*T*A*A. As a non-targeting negative control, the following GapmeR sequence was used: A*A*C*A*C*G*T*C*T*A*T*A*C*G*C. Knockdowns were performed at least three times in each cell line.

Cell proliferation and cytotoxicity assays

Cell viability was measured at 48-, 72- and 96-h post-transfection according to the manufacturer's protocol (EZ4U; Biomedica Group, Vienna, Austria). The absorbance of a viability-dependent derivative as a surrogate for cell proliferation was measured using a microplate reader. Each experiment was performed in triplicates.

Migration assays

5000 cells were plated in the upper chamber of the migration inserts (VWR, Darmstadt, Germany) containing 2% FCS medium, whereas the lower chamber was filled with a medium containing 10% FCS for chemotactic attraction. After 24 h of incubation, cells were fixed with 4%

Table 1
Multivariate Cox regression analyses in the evaluated KIRC cohorts regarding overall survival (OS).

Multivariate Cox regression analyses [TNM, age]		
Clinical-pathological parameters	p value	Hazard ratio [95% CI low/high]
KIRC TCGA cohort (RNAseq)		
DONSON mRNA	< 0.0001	2.27 [1.68; 3.07]
T-stage	0.001	1.03 [1.01; 1.05]
N-stage	0.07	1.27 [0.98; 1.65]
M-stage	0.54	1.24 [0.62; 2.50]
Age	< 0.0001	2.89 [1.76; 4.75]
KIRC cDNA cohort (qPCR)		
DONSON mRNA	0.04	2.36 [1.04; 5.37]
T-stage	0.54	1.16 [0.73; 1.84]
N-stage	0.72	0.76 [0.18; 3.29]
M-stage	0.01	3.46 [1.32; 9.08]
Age	0.02	1.06 [1.01; 1.12]
KIRC TMA cohort (IHC)		
DONSON protein	0.05	2.95 [1.00; 8.69]
T-stage	0.21	1.45 [0.81; 2.59]
N-stage	0.61	1.10 [0.75; 1.60]
M-stage	0.43	1.21 [0.75; 1.96]
Age	0.60	1.01 [0.97; 1.06]

formaldehyde and stained with hematoxylin. Membranes were scanned, and cells were counted automatically by nucleus detection using the QuPath software [21]. Each experiment was performed in triplicates.

Statistical analysis

SPSS Statistics v25, Microsoft Excel, and GraphPad Prism Version 8.2.1 were used for statistics. Group comparisons were performed using the nonparametric Mann-Whitney-U or Kruskal–Wallis test. Uni-/multivariate Cox regression analyses [TNM; Age] and Kaplan Meier estimates were performed to evaluate the prognostic value of the DONSON [22,23].

Results

Pan-cancer analyses of DONSON using TCGA datasets

To comprehensively investigate the general prognostic potential of *DONSON*, we performed a systematic pan-cancer survival analysis for 30 different tumor entities of TCGA (N = 9022; Fig. 1A + B). Interestingly, *DONSON* overexpression was preferentially associated with poor survival in 9 of the 30 entities, suggesting tumor-independent oncogenic properties for this gene (Fig. 1A + B). Especially in KIRC, adrenocortical carcinoma (ACC) and mesothelioma (MESO) *DONSON* was strongly associated with an unfavorable OS ($p < 0.0001$). It has to be mentioned that *DONSON* overexpression was also associated with unfavorable OS in other frequently occurring tumor entities, which is of particular interest as most of these tumors do not share similar phenotypes or phylogenetic features. Of note, DONSON has not been investigated in all of these cancers so far. As the second most common subtype of RCC, KIRP also showed an association between an aggressive phenotype and enhanced *DONSON* expression ($p = 0.002$). In multivariate Cox regression analyses, *DONSON* was found to be the strongest independent predictor of unfavorable OS in KIRC compared to all other investigated entities (Hazard Ratio (HR) 2.3, 95% CI; 1.7–3.1; $p < 0.0001$, Table 1). This strong association prompted us to investigate the role of DONSON in KIRC more comprehensively. By comparing the *DONSON* mRNA expression in KIRC to normal adjacent renal tissue (NAT), we observed a significant upregulation in the tumor samples (Fig. 2A). Advanced pathological T-stages, lymphonodal, and distant metastatic spread, known as the critical steps during RCC progression, were also

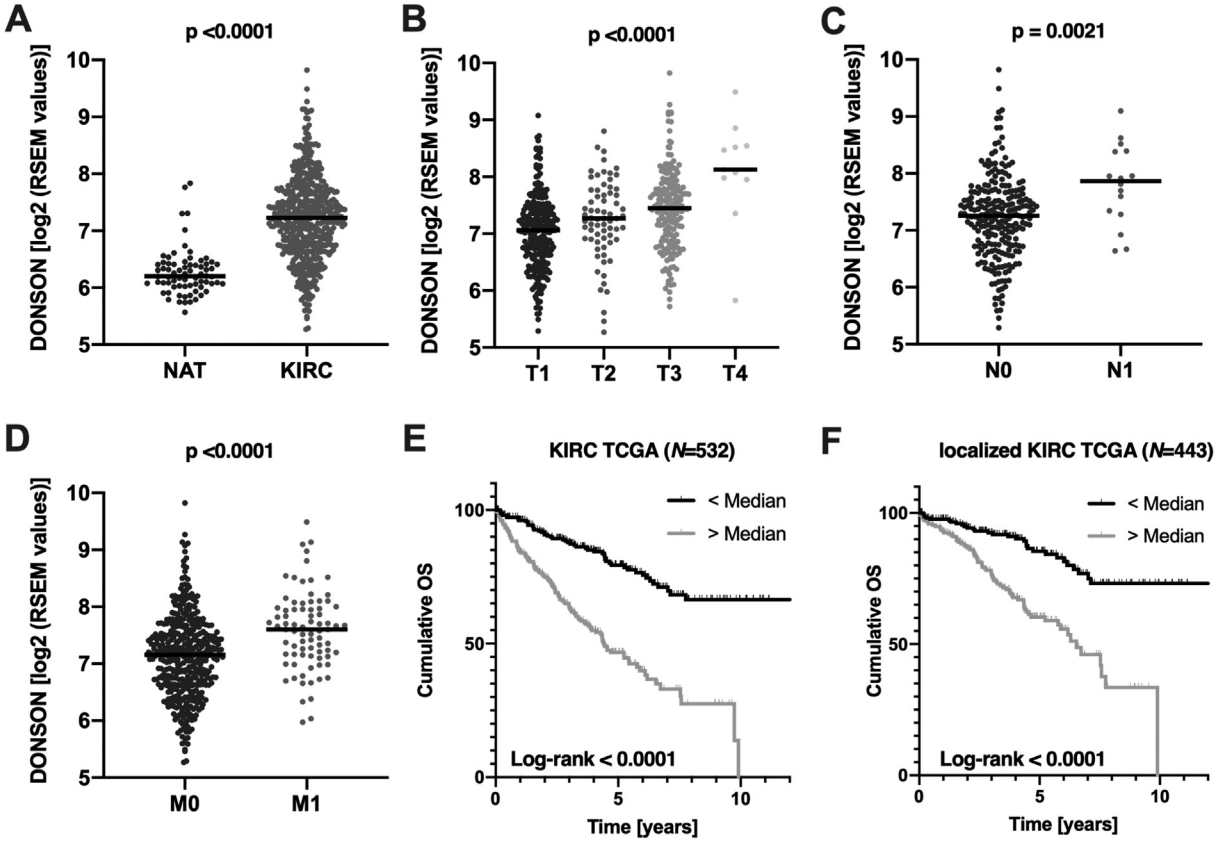

Fig. 2. Association of DONSON with pathological parameters and survival using the KIRC TCGA dataset A: DONSON expression in KIRC vs normal adjacent kidney tissue (NAT). Association of DONSON expression with TNM-Staging (B–D). E, Survival analysis following the dichotomization of the whole (E) as well as only the localized KIRC (F) cohort based on the median DONSON mRNA expression.

strongly associated with increased *DONSON* mRNA expression (Fig. 2B–D). Significantly reduced OS was seen in the group of *DONSON* overexpressing tumors (Fig. 2E). Of note, also in the group of localized KIRC ($N = 443$, Fig. 2F), *DONSON* showed a strong association with shortened OS, which may be a hint for the value of *DONSON* for risk stratification in the non-metastatic setting.

DONSON mRNA expression in an independent KIRC cDNA cohort

In accordance with the TCGA results, we detected significantly increased *DONSON* mRNA expression in KIRC compared to NAT (Fig. 3A). Further, *DONSON* overexpressing KIRC was associated with a significantly reduced overall (OS), cancer-specific (CSS) and progression-free survival (PFS) (Fig. 3B–D). After adjusting the co-variates TNM stage and age at initial diagnosis, we found that DONSON represents an independent risk factor for reduced OS (HR 2.4, 95% CI; 1.0–5.4; $p = 0.04$, Table 1) and CSS (HR 3.0, 95% CI; 1.1–8.0; $p = 0.03$, Table 1) in our KIRC cDNA cohort. Hence, we were able to validate the prognostic potential of *DONSON* in an independent RCC cohort on the transcriptional level.

DONSON protein expression on RCC TMA

We have further investigated a clinically annotated RCC tissue microarray (TMA) by immunohistochemical staining against DONSON to test its potential as a prognostic biomarker at the protein level. We observed preferentially cytoplasmatic staining against DONSON, which is in line with the staining pattern of DONSON in the RCC cohort of The Human Protein Atlas (HPA, www.proteinatlas.org; [24]). In the non-cancerous renal cortex, the proximal tubules exhibited the strongest DONSON expression (Fig. 4A). DONSON protein expression was again higher in KIRC than in NAT (Fig. 4B) in accordance with the transcriptional upregulation in the TCGA and cDNA cohorts. Further, we performed Western Blots for DONSON on 8 paired formalin-fixed paraffin-embedded paraffin (FFPE) KIRC and NAT tissue samples. Six of the eight matched specimens presented noticeably higher DONSON expression compared to NAT, and only one sample vice versa (Fig. 4C).

In KICH, DONSON expression was low, whereas the KIRP subtype showed the strongest DONSON expression across the RCC subtypes (Fig. 4A + D). The differential DONSON expression between KICH, KIRC, and KIRP was similar at the transcriptional level using the TCGA datasets. KICH showed the lowest DONSON expression levels, followed by KIRC, whereby KIRP exhibited the strongest DONSON expression (Fig. 4D + E). Interestingly, KIRC exhibited a heterogeneous DONSON expression throughout the cohort, with a negative as well as a DONSON-overexpressing subgroup (Fig. 4A). Consistent with DONSON's prognostic value seen on the transcriptional level, this DONSON-overexpressing subgroup showed a significantly reduced progression-free (PFS) and overall survival (OS) (Fig. 4E + F). Of particular interest is that DONSON overexpression on the protein level was again shown to be an independent predictor of both unfavorable PFS (HR 3.1, 95% CI; 1.2–8.3; $p = 0.02$, Table 1) and OS (HR 2.9, 95% CI; 1.0–8.7;

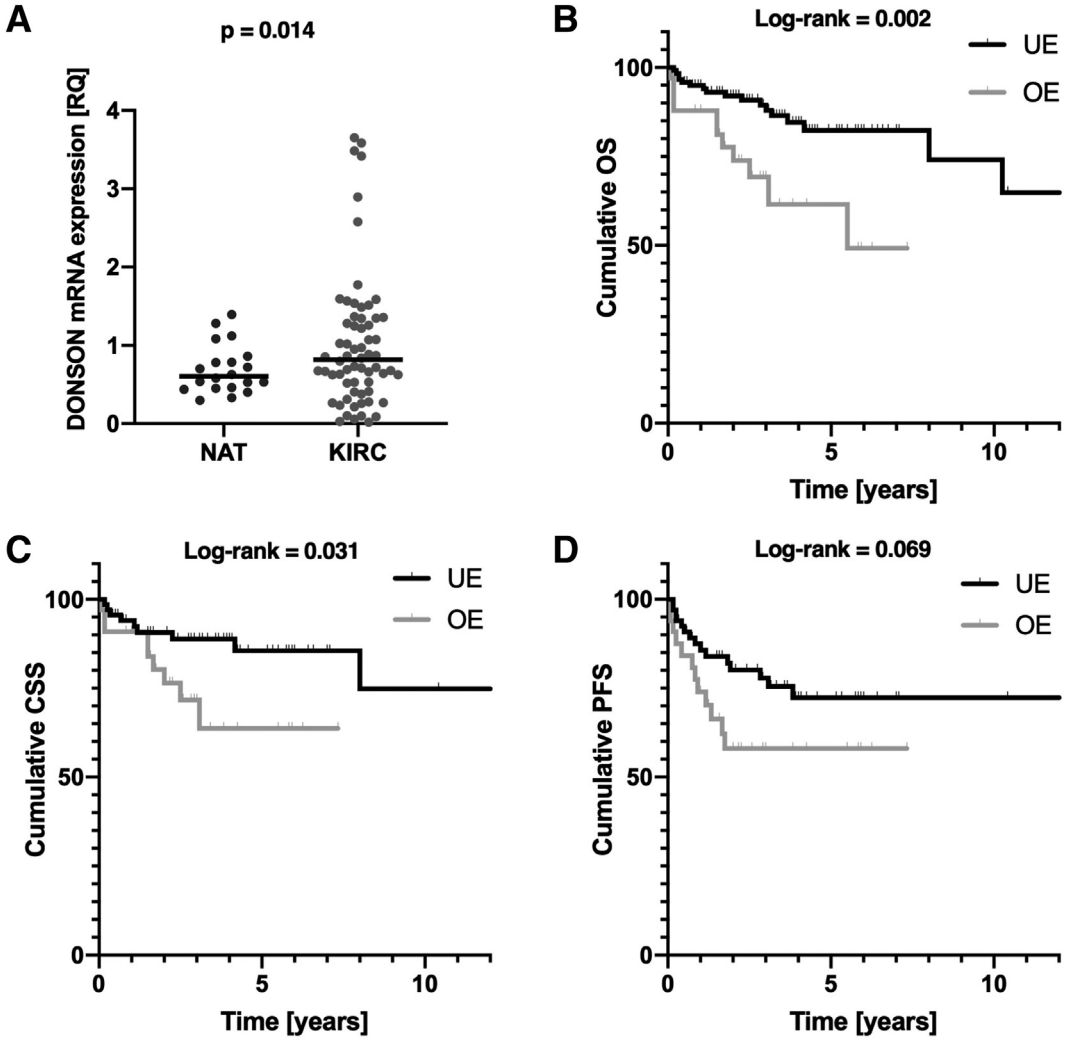

Fig. 3. A, DONSON mRNA level is increased in KIRC vs normal adjacent kidney tissue (NAT). B–D Using an optimized cutoff, tumors overexpressing DONSON ($N = 34$) are correlated with unfavorable overall (B, OS), cancer-specific (C, CSS) and progression-free survival (D, PFS) compared to tumors with low DONSON mRNA expression ($N = 69$).

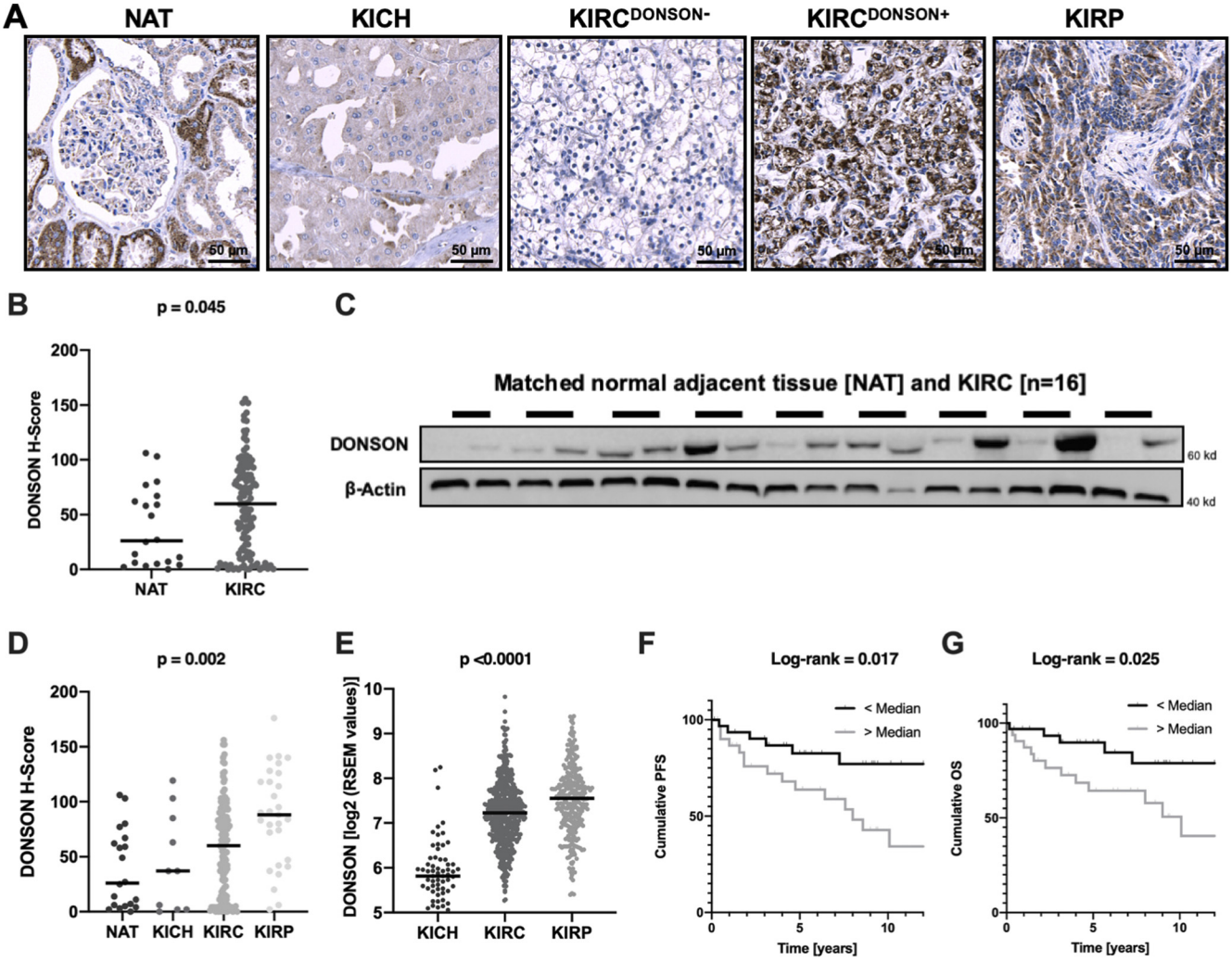

Fig. 4. IHC staining of DONSON on an RCC tissue microarray with subsequent software-based expression analysis A, Representative images of DONSON IHC staining for kidney tissue (normal adjacent tissue, NAT), chromophobe RCC (KICH), DONSON-negative/positive KIRC, and papillary RCC (KIRP) tissue samples, 10× objective magnification. B + C, DONSON protein expression is upregulated during tumor formation of KIRC compared to NAT assessed on the TMA cohort (B) and via Western Blotting of 8 matched pairs NAT vs KIRC (C). D + E Differential DONSON expression across the three most common RCC subtypes examined on the TMA cohort (D) and via the TCGA datasets for KICH ($N = 66$), KIRC ($N = 532$) and KIRP ($N = 290$) (E). DONSON overexpressing tumors are associated with unfavorable progression-free and overall survival.

$p = 0.05$, Table 1) measured by a multivariate Cox regression co-adjusting the TNM stage and age at initial diagnosis. In metastatic KIRC, DONSON expression was enhanced, although lacking a statistical significance, which might be due to the low sample size (Suppl. Fig. 1A, M1 $N = 15$, $p = 0.15$). DONSON overexpression was associated with high-grade KIRC histopathology, nonetheless only a trend towards statistical significance was seen (Suppl. Fig. 1B $p = 0.12$).

In total, DONSON as an independent predictor of unfavorable OS on both transcriptional and translational levels in three distinct RCC cohorts represents a promising and robust prognostic biomarker for risk stratification of our KIRC patients.

Functional in vitro analyses of DONSON

In order to evaluate the role DONSON plays in tumor progression and metastasis, we conducted in-vitro investigations in established RCC cell culture models. All evaluated RCC cell lines - ACHN, Caki1 and 769p - express DONSON protein in similar amounts (Fig. 5A). We induced specific DONSON-knockdowns via transfection of antisense oligonucleotides (Antisense LNA-GapmeR system) and established efficient knockdowns assessed by qRT-PCR (Fig. 5B). Western Blot analyses also confirmed efficient knockdowns on the translational level in all three evaluated cell lines (Fig. 5C). Thereafter, we investigated the effect of specific DONSON depletion on the proliferative activity of the RCC cells compared to negative control. We observed inhibition of cell proliferation in a time-dependent manner over a time course of 96 h post-transfection with significantly impaired proliferation observed for Caki1 and 769p (Fig. 5D). Moreover, in Caki1 and 769p, depletion of DONSON led to significantly attenuated migration capacities measured by Boyden Chamber Migration assays (Fig. 5E + F), whereas only a trend was seen in the ACHN cell lines without statistical significance reached ($p = 0.19$).

We concluded that DONSON expression in the KIRC cell culture model is necessary to maintain the malignant potential in vitro. Thus, DONSON could serve as an interesting therapeutic target.

Discussion

In this study, in a comprehensive pan-cancer analysis, we were able to associate the largely unknown gene *DONSON* with unfavorable OS in a variety of solid tumors (Fig. 1). *DONSON*, therefore, seems to be cancer-type independently associated with aggressive phenotype and thus is a highly promising gene for further basic and oncological research. The strongest

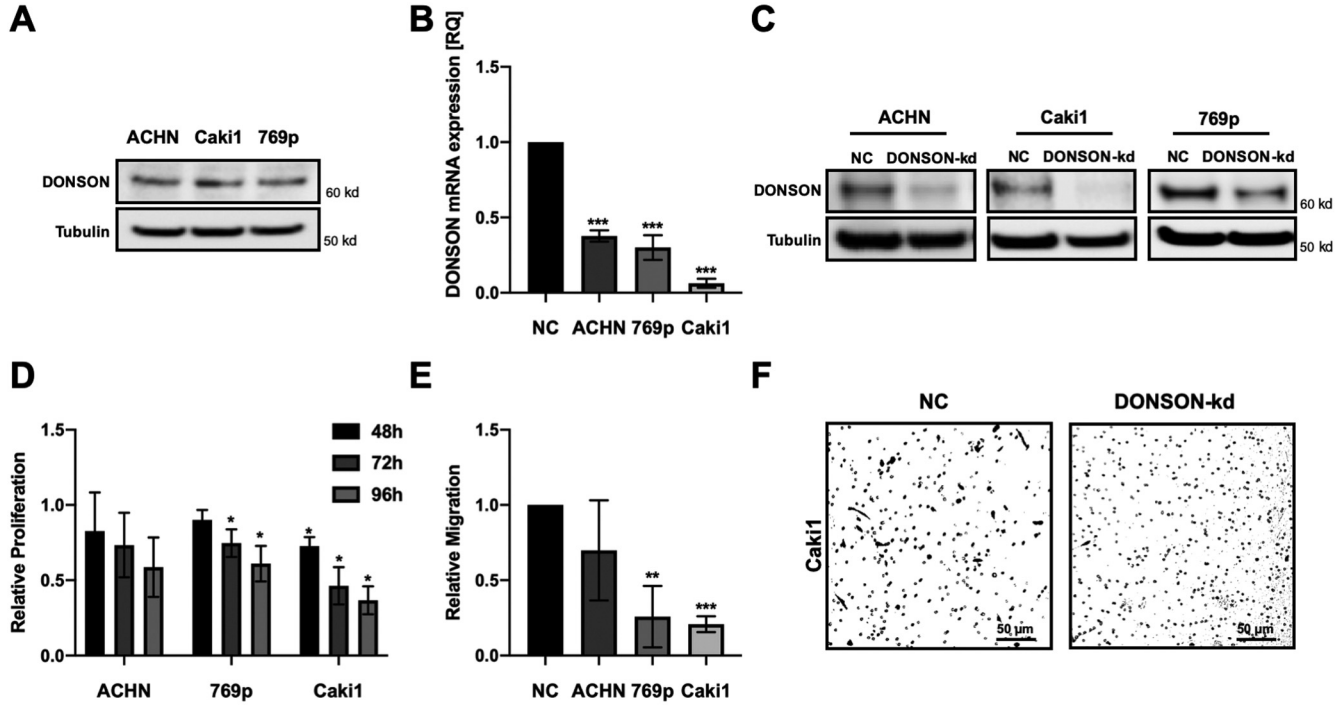

Fig. 5. Functional analyses of DONSON in the renal cancer cell lines ACHN, Caki1 and 769p. A, Screening Western Blot for DONSON. B + C An efficient Antisense LNA GapmeR-mediated DONSON knockdown was induced and validated via qPCR (B) and Western Blotting (C). D DONSON-depletion led to significantly reduced viability in Caki1 and 769p in a time-dependent manner. E + F Migration capacity (E + F) was strongly reduced after DONSON-depletion, especially prominent in Caki1 (F), 10× objective magnification.

association between poor survival and *DONSON* overexpression was found in KIRC, which was consequently selected for further analyses. Thus, the robust expression data of the KIRC TCGA cohort could be validated in two further independent RCC cohorts on the transcriptional and translational level, which highlights its robustness as a promising biomarker [22].

We hypothesized that genes that show a strong correlation to unfavorable survival, and therefore to particularly aggressive tumors, represent interesting targets for further research. Thus, we have investigated DONSON's functional role in established RCC cell culture models. In our cell culture model, the depletion of DONSON caused a decrease in the proliferative activity and an attenuation of the migration capacities of CAKI1 and 769p KIRC cells. Recently, the tumor-suppressive miR-101-5p was shown to negatively regulate DONSON and several replisome genes in KIRC. Expression of miR-101-5p, as well as siRNA-mediated DONSON knockdown, caused cell cycle arrest, apoptosis, and impaired motility in the RCC cell lines 786O and A498 [16]. Our results are, therefore, in line with this previously published study.

Chemotherapeutic agents play an essential role in the therapy of many tumors. These drugs especially interfere with metabolic processes associated with cell growth or cell division. Tumor cells have an increased cell division rate as well as limited DNA damage repair capacity, which is why they are more sensitive to these drugs than healthy cells. DONSON could be an interesting targeted therapeutic target as it plays a vital role in both cellular processes, replication, and maintaining genome stability [14,15]. It is an essential gene for stable replication forks during S-phase and thus for proliferation itself and plays a pivotal role in maintaining genomic integrity and stability. It could, therefore, serve as a promising target in the therapy of various tumors (Fig. 1), where DONSON inhibition could restrict proliferation while negatively affecting the genomic integrity of the tumor cell, which ultimately could lead to tumor shrinkage. Our functional investigations already underline this hypothesis as DONSON-depletion caused growth restriction in a time-dependent manner in our RCC cell culture model. This is in line with previous literature, where DONSON-depletion also induced apoptosis [16]. Nevertheless, it should be mentioned that DONSON's potential as a therapeutic target requires further investigation. However, our study, which associates DONSON with an aggressive phenotype in multiple tumor types, could be a starting point for further basic and oncological research on DONSON and may open the avenue for DONSON being an attractive therapeutic target.

Conclusion

In total, we were able to associate the widely unknown gene *DONSON* with poor overall survival in various solid tumors. In particular, we identify DONSON as an interesting biomarker for risk stratification in KIRC in three independent cohorts and provide evidence that DONSON is linked to a malignant phenotype in the RCC cell culture model.

Supplementary data to this article can be found online at https://doi.org/10.1016/j.tranon.2020.100844.

Authorship

Niklas Klümper: Conceptualization, Methodology, Software, Validation, Formal analysis, Investigation, Writing – original draft, Visualization, Funding acquisition
Iulia Blajan: Investigation, Writing – review & editing, Visualization
Doris Schmidt: Investigation, Writing – review & editing
Glen Kristiansen: Investigation, Resources, Writing – review & editing
Marieta Toma: Investigation, Resources, Writing – review & editing
Michael Hölzel: Investigation, Resources, Writing – review & editing
Manuel Ritter: Resources, Project administration, Writing – review & editing, Funding acquisition
Jörg Ellinger: Supervision, Resources, Project administration, Writing – review & editing, Funding acquisition.

Declaration of competing interest

The authors declare that they have no known competing financial interests or personal relationships that could have appeared to influence the work reported in this paper.

Acknowledgements

The tissue samples were collected within the framework of the Biobank of the Center for Integrated Oncology Cologne Bonn at the University Hospital Bonn. All patients gave written informed consent for the collection of biomaterials. The study was approved by the ethics committee at the University Hospital Bonn (number: 273/18). This study was supported by a Ferdinand Eisenberger grant of the Deutsche Gesellschaft für Urologie (German Society of Urology), grant ID KIN1/FE-19 (NK) and the BONFOR Program of the medical faculty of the University of Bonn (IB), grant ID 2019-4-05 (IB).

References

[1] R.L. Siegel, K.D. Miller, A. Jemal, Cancer statistics, 2019, CA Cancer J. Clin. 69 (1) (2019) 7–34.
[2] F. Bray, J. Ferlay, I. Soerjomataram, R.L. Siegel, L.A. Torre, A. Jemal, Global cancer statistics 2018: GLOBOCAN estimates of incidence and mortality worldwide for 36 cancers in 185 countries, CA Cancer J. Clin. 68 (6) (2018 Nov) 394–424.
[3] B.I. Rini, S.C. Campbell, B. Escudier, Renal cell carcinoma, Lancet 373 (9669) (2009 Mar) 1119–1132.
[4] R.J. Motzer, B.I. Rini, D.F. McDermott, O. Arén Frontera, H.J. Hammers, M.A. Carducci, et al., Nivolumab plus ipilimumab versus sunitinib in first-line treatment for advanced renal cell carcinoma: extended follow-up of efficacy and safety results from a randomised, controlled, phase 3 trial, Lancet Oncol. 16 (2019 Aug).
[5] B.I. Rini, E.R. Plimack, V. Stus, R. Gafanov, R. Hawkins, D. Nosov, et al., Pembrolizumab plus axitinib versus sunitinib for advanced renal-cell carcinoma, N. Engl. J. Med. 380 (12) (2019 Mar 21) 1116–1127.
[6] B. Ljungberg, L. Albiges, Y. Abu-Ghanem, K. Bensalah, S. Dabestani, S. Fernández-Pello, et al., European Association of Urology guidelines on renal cell carcinoma: the 2019 update, Eur. Urol. 75 (5) (2019) 799–810.
[7] L. Albiges, T. Powles, M. Staehler, K. Bensalah, R.H. Giles, M. Hora, et al., Updated European Association of Urology guidelines on renal cell carcinoma: immune checkpoint inhibition is the new backbone in first-line treatment of metastatic clear-cell renal cell carcinoma, Eur. Urol. 76 (2) (2019 Aug 1) 151–156.
[8] R.J. Motzer, K. Penkov, J. Haanen, B. Rini, L. Albiges, M.T. Campbell, et al., Avelumab plus axitinib versus sunitinib for advanced renal-cell carcinoma, N Engl J Med. 380 (12) (21 2019) 1103–1115.
[9] The Cancer Genome Atlas Research Network, J.N. Weinstein, E.A. Collisson, G.B. Mills, K.R.M. Shaw, B.A. Ozenberger, et al., The Cancer Genome Atlas Pan-Cancer analysis project, Nat. Genet. 45 (2013 Sep 26) 1113–1120.
[10] J. Gao, B.A. Aksoy, U. Dogrusoz, G. Dresdner, B. Gross, S.O. Sumer, et al., Integrative analysis of complex cancer genomics and clinical profiles using the cBioPortal, Sci Signal. 6 (269) (Apr 2 2013) pl1.
[11] F. Sanchez-Vega, M. Mina, J. Armenia, W.K. Chatila, A. Luna, K.C. La, et al., Oncogenic signaling pathways in The Cancer Genome Atlas, Cell 173 (2) (05 2018) 321–337.e10.
[12] Cancer Genome Atlas Research Network, Comprehensive molecular characterization of clear cell renal cell carcinoma, Nature. 499 (7456) (Jul 4 2013) 43–49.
[13] J. Anaya, OncoLnc: linking TCGA survival data to mRNAs, miRNAs, and lncRNAs, PeerJ Comput. Sci. 2 (Jun 13 2016), e67.
[14] J.J. Reynolds, L.S. Bicknell, P. Carroll, M.R. Higgs, R. Shaheen, J.E. Murray, et al., Mutations in DONSON disrupt replication fork stability and cause microcephalic dwarfism, Nat. Genet. 49 (4) (2017 Apr) 537–549.
[15] F. Fuchs, G. Pau, D. Kranz, O. Sklyar, C. Budjan, S. Steinbrink, et al., Clustering phenotype populations by genome-wide RNAi and multiparametric imaging, Mol. Syst. Biol. 6 (Jun 8 2010) 370.
[16] Y. Yamada, N. Nohata, A. Uchida, M. Kato, T. Arai, S. Moriya, et al., Replisome genes regulation by antitumor miR-101-5p in clear cell renal cell carcinoma, Cancer Sci. 111 (4) (Jan 23 2020) 1392–1406, https://doi.org/10.1111/cas.14327.
[17] A. Strick, F. von Hagen, L. Gundert, N. Klümper, Y. Tolkach, D. Schmidt, et al., The N6-methyladenosine (m6 A) erasers alkylation repair homologue 5 (ALKBH5) and fat mass and obesity-associated protein (FTO) are prognostic biomarkers in patients with clear cell renal carcinoma, BJU Int. 27 (2020 Jan).
[18] M. Brüggemann, A. Gromes, M. Poss, D. Schmidt, N. Klümper, Y. Tolkach, et al., Systematic analysis of the expression of the mitochondrial ATP synthase (complex V) subunits in clear cell renal cell carcinoma, Transl. Oncol. 10 (4) (2017 Aug) 661–668.
[19] N. Klümper, I. Syring, A. Offermann, Z. Shaikhibrahim, W. Vogel, S.C. Müller, et al., Differential expression of mediator complex subunit MED15 in testicular germ cell tumors, Diagn. Pathol. 10 (1) (Sep 17 2015) 165.
[20] N. Klümper, I. Syring, W. Vogel, D. Schmidt, S.C. Müller, J. Ellinger, et al., Mediator complex subunit MED1 protein expression is decreased during bladder cancer progression, Front. Med. 4 (2017) 30.
[21] P. Bankhead, M.B. Loughrey, J.A. Fernández, Y. Dombrowski, D.G. McArt, P.D. Dunne, et al., QuPath: open source software for digital pathology image analysis, Sci. Rep. 7 (1) (2017 Dec) 16878.
[22] L.M. McShane, D.G. Altman, W. Sauerbrei, S.E. Taube, M. Gion, G.M. Clark, et al., REporting recommendations for tumour MARKer prognostic studies (REMARK), Br. J. Cancer 93 (4) (2005 Aug 22) 387–391.
[23] R.M. Simon, S. Paik, D.F. Hayes, Use of archived specimens in evaluation of prognostic and predictive biomarkers, J. Natl. Cancer Inst. 101 (21) (2009 Nov 4) 1446–1452.
[24] M. Uhlen, C. Zhang, S. Lee, E. Sjöstedt, L. Fagerberg, G. Bidkhori, et al., A pathology atlas of the human cancer transcriptome, Science 357 (6352) (Aug 18 2017), eaan2507.